Environ Sci Pollut Res (2017) 24:4791–4800
DOI 10.1007/s11356-016-8138-3

RESEARCH ARTICLE

Photo-Fenton and Fenton-like processes for the treatment of the antineoplastic drug 5-fluorouracil under simulated solar radiation

A. Koltsakidou [1] · M. Antonopoulou [2] · M. Sykiotou [1] · E. Evgenidou [1] · I. Konstantinou [3] · D.A. Lambropoulou [1]

Received: 2 August 2016 / Accepted: 21 November 2016 / Published online: 16 December 2016

Abstract In the present study, photo-Fenton and Fenton-like processes were investigated for the degradation and mineralization of the antineoplastic drug 5-fluorouracil (5-FU). For the optimization of photo-Fenton treatment under simulated solar light (SSL) radiation, the effects of several operating parameters (i.e., 5-FU concentration, Fe^{3+}, and oxidant concentration) on the treatment efficiency were studied. According to the results, SSL/$[Fe(C_2O_4)_3]^{3-}$/H_2O_2 process was the most efficient, since faster degradation of 5-FU and higher mineralization percentages were achieved. All the applied processes followed quite similar transformation routes which include defluorination-hydroxylation as well as pyrimidine ring opening, as demonstrated by the transformation products identified by high resolution mass spectrometry analysis. The toxicity of the treated solutions was evaluated using the Microtox assay. In general, low toxicity was recorded for the initial solution and the solution at the end of the photocatalytic treatment, while an increase in the overall toxicity was observed only at the first stages of SSL/Fe^{3+}/H_2O_2 and SSL/Fe^{3+}/$S_2O_8^{2-}$ processes.

Responsible editor: Philippe Garrigues

✉ D.A. Lambropoulou
dlambro@chem.auth.gr

[1] Department of Chemistry, Aristotle University of Thessaloniki, 54124 Thessaloniki, Greece

[2] Department of Environmental and Natural Resources Management, University of Patras, 30100 Agrinio, Greece

[3] Department of Chemistry, University of Ioannina, 45110 Ioannina, Greece

Keywords 5-fluorouracil · Pharmaceuticals · Photo-Fenton · Fenton-like processes · AOPs · Toxicity · Transformation products

Introduction

Antineoplastic ("anticancer" or "cytostatic") drugs are one of the main chemotherapeutic agent families widely used in the fight against cancer (Lutterbeck et al. 2015a). They have been shown to have potent genotoxic, cytotoxic, carcinogenic, mutagenic, teratogenic, and/or endocrine disruptor effects on several organisms, since they have been designed to disrupt or prevent cellular proliferation, usually by interfering in DNA synthesis (Ferrando-Climent et al. 2015).

These substances are mostly discharged into the environment through the excretion of urine and feces from chemotherapy patients. Under controlled situations, they are administered at hospitals and lately at home by outpatients' (Besse et al. 2012). Because of this ongoing move towards outpatient treatment and the fact that hospital effluent often leads into the municipal sewer system, municipal wastewater would now be an important source for the introduction of these drugs into the environment (Toolaram et al. 2014). Although the measured environmental concentrations of these compounds are lower than those of more commonly used pharmaceuticals (Parrella et al. 2015), the antineoplastic drugs are of particular environmental concern, since even at trace levels they have been suggested to have a capacity to cause pronounced environmental effects (Ferrando-Climent et al. 2014, Parrella et al. 2014a).

One of the most commonly administered antineoplastic drugs is 5-fluorouracil (5-FU), while several studies have shown evidence for its presence in different water compartments, mostly in hospital and municipal wastewaters, in

concentrations ranging from nanogram per liter up to microgram per liter (Catastini et al. 2008, Kosjek et al. 2013, Mahnik et al. 2007, Weissbrodt et al. 2009). 5-FU is an antimetabolite that exerts its anticancer effects through inhibition of DNA synthesis and replication, by inhibition of thymidylate synthase, and by incorporation of 5-FU metabolites into RNA and DNA (Kovács et al. 2015). Research has shown that 60–90% of the taken 5-FU is metabolized and then excreted, while the remaining 10–30% is excreted as the parent form that enters hospital or municipal wastewater (Straub 2010). More and more investigations are conducted lately, studying the toxicity of 5-FU, indicating the importance to develop efficient treatment methods to degrade 5-FU and to investigate the nature of transformation of this drug in water treatment processes (Brezovšek et al. 2013, 2014, Kovács et al. 2015, Parrella et al. 2014a, Parrella et al. 2014b).

Advanced oxidation processes (AOPs) have been studied as an alternative option for treating many types of industrial and municipal wastewater (Papoutsakis et al. 2015). AOPs have successfully mineralized or converted persistent micropollutants to less harmful forms (Ikehata et al. 2006). Although the hydroxyl radical ($HO^{\bullet}$) is the main oxidizing agent in these processes, their application often induces the production and participation of other reactive oxygen species (ROS), such as superoxide radical anions, hydroperoxyl radicals, and singlet oxygen (Giannakis et al. 2015). The characteristic versatility of the oxidation processes is one the main advantages for their applications (De la Cruz et al. 2012).

So far, the degradation of 5-FU was studied by photolysis under UV light or simulated sunlight (Lin et al. 2013, Miolo et al. 2011) while Lutterbeck et al. (2015b) and Lin and Lin (2014) applied different advanced photo-oxidation processes (Lin & Lin 2014, Lutterbeck et al. 2015b). Lutterbeck et al. (2015b) investigated 5-FU degradation by UV/H_2O_2, UV/$Fe^{2+/}H_2O_2$ and UV/TiO_2, achieving the highest degree of mineralization processes by UV/Fe^{2+}/H_2O_2, and UV/TiO_2. Lin and Lin (2014) applied heterogeneous photocatalysis under UV irradiation, using several semiconductors (ZnO, Degussa P25, Aldrich-TiO_2) as photocatalysts and concluded that Degussa P25 exhibited the highest activity.

Bearing in mind the need for further investigation on the effectiveness of AOPs for the degradation of 5-FU, the present work aims to study the application of three different AOPs (homogeneous photocatalysis), under simulated solar irradiation. The main objectives for this study were: (i) the comparison of photo-Fenton (Fe^{3+}/H_2O_2) and photo-Fenton-like ($[Fe(C_2O_4)_3]^{3-}/H_2O_2$, $Fe^{3+}/S_2O_8{}^{2-}$) treatments under simulated solar irradiation for the degradation of 5-FU, (ii) the evaluation of the efficiency of each treatment for the elimination of 5-FU by means of mineralization, and (iii) the identification and comparison of the transformation products (TPs) formed during the studied processes.

Materials and methods

Reagents and materials

5-FU, analytical grade > 99%, was obtained from TCI (TOKYO Chemical Industry CO). LC-MS-grade solvents (methanol, and water) were supplied by Fisher Scientific. The salts used for the oxidation techniques were iron(III) chloride hexahydrate ($FeCl_3{\cdot}6H_2O$, 99%), sodium persulfate ($Na_2S_2O_8$, 99+%), and potassium oxalate monohydrate ($C_2K_2O_4{\cdot}1H_2O$, 99.5+%), all purchased from Chem-Lab NV (Zedelgem, Belgium). Hydrogen peroxide (H_2O_2, 30% *w*/*v*) was obtained from Panreac (Barcelona, Spain). Sodium carbonate (Na_2CO_3) and sodium hydrogen carbonate ($NaHCO_3$), used for ion chromatography analyses, were obtained from Sigma–Aldrich (Germany). Ultrapure water used for the experiments was obtained from Millipore Waters Milli-Q water purification system.

Photo-Fenton experiments

The photo-Fenton experiments were carried out in a solar simulator Atlas Suntest CPS+ (Germany) equipped with a xenon lamp (1.5 kW) using a constant irradiance of 500 W m^{-2} (measured by a calibrated internal radiometer of the Suntest apparatus). The spectrum of the Xenon lamp with the used filters is presented elsewhere (Weber et al. 2009).

In each experiment, 100 mL of 5-FU solution (10 mg L^{-1}, unless otherwise stated) was mixed with the appropriate amount of iron (0–4.5 mg L^{-1}) in a double-walled Pyrex glass reactor, thermostated by a water circuit and magnetically stirred before and during the illumination. At the beginning of the experiments, 5-FU solutions were acidified (pH was adjusted to 2.9–3 in all cases) using HCl. Acidic pH was selected since optimal Fenton and photo-Fenton processes require pH values ≤3, in order to prevent the iron precipitation as $Fe(OH)_3$. The reaction was initiated by adding the appropriate amount of hydrogen peroxide (0–90 mg L^{-1}).

Photo-Fenton like processes

Fenton-like ($Fe^{3+}/S_2O_8{}^{2-}$, $[Fe(C_2O_4)_3]^{3-}/H_2O_2$) photocatalysis was carried out in the solar simulator described previously in the "Photo-fenton experiments" section. The pH of 5-FU solution was adjusted to 2.8 with HCl. The concentration of Fe^{3+} and the used oxidant were 4.5 and 100 mg L^{-1}, respectively. Ferrioxalate ($[Fe(C_2O_4)_3]^{3-}$) was prepared as a mixture containing a 1:3 M ratio of iron(III) chloride hexahydrate ($FeCl_3{\cdot}6H_2O$) and potassium oxalate monohydrate ($C_2K_2O_4{\cdot}1H_2O$), prior to each experiment. With a view to achieve not very fast degradation kinetics of 5-FU, which will favor the identification of TPs as well as the determination of

mineralization's evolution, 30 mg L^{-1} (200 mL solution) of 5-FU was used as initial concentration.

Analytical procedures

Kinetic studies

An HPLC system (SIL 20A autosampler and a LC-20AB pump both from Shimadzu, Kyoto, Japan) with a SPD 20A DAD detector coupled in series with a 2010EV mass spectrometry detector, equipped with an atmospheric pressure electrospray ionization source (ESI), was used for the quantification of 5-FU, during the applied processes. The analysis was performed on a C_{18}, 150 × 4.6 mm with 3.5-μm particle size (Pathfinder) analytical column, thermostated at 40 °C. The mobile phase was a mixture of LC-MS grade water −0.1% formic acid (60%) and LC-MS grade methanol (40%) with a flow rate of 0.4 mL min^{-1}. The total run analysis lasted 6 min and the injection volume was adjusted at 20 μL. The samples were analyzed in negative ionization (NI) mode and the precursor molecular ion $[M-H]^-$ in the selected-ion monitoring (SIM) mode was acquired (129 m/z) for 5-FU. The mass spectrometer was operated under the following conditions: drying gas 10 L min^{-1}, temperature 200 °C, nebulizing pressure 100 psi, capillary voltage −3500 V, and fragmentation voltage 1.65 V.

Mineralization studies

The mineralization percentages achieved during the applied processes were evaluated by dissolved organic carbon (DOC) measurements, performed on a Shimadzu TOC V-csh Analyzer. NO_3^- and F^- ions were quantified by an ion chromatography (Metrohm) equipped with an automatic sampler and a Metrosep A Supp 4 (250 mm x 4.0 mm) with 9 μm particle size analytical column. A mixture of Na_2CO_3 1.8 mM–$NaHCO_3$ 1.7 mM with a flow rate of 1 mL min^{-1} was used as an eluent. The duration of chromatographic program was 20 min, while the injection volume was 20 μL.

Transformation products evaluation

The identification of TPs was performed on a LC-TOF-MS system (Bruker micrOTOF Focus II connected to a Dionex UHPLC Ultimate 3000) described in detail previously (Antonopoulou et al. 2016). The mobile phase was LC-MS grade water with 0.01% formic acid (A) and LC-MS grade methanol (B) at a flow rate of 0.3 mL/min. The gradient elution was started with 1% methanol and increased linearly to 99% at 6.0 min and then reverted to 1% methanol at 10.0 min. Finally, 2 min was set as equilibration time. The chromatographic program lasted 12 min. The injection volume was 20 μL. MS analysis for the TPs' identification was performed in both positive (set capillary at 4000 V) and negative ionization mode (set capillary at 4200 V). The other conditions adopted in the mass spectrometer part using otofControl software are similar to those presented in a previous work (Antonopoulou et al. 2016).

Toxicity evaluation

Acute toxicity (% inhibition of the *Vibrio fischeri* luminescence in 15 min of incubation) of the treated samples was estimated using a Microtox Model 500 Toxicity Analyzer as described previously (Antonopoulou & Konstantinou 2014). Samples were taken at the beginning, at the first stages and at the end of each procedure. Sodium thiosulphate was used as a quenching factor in stoichiometric doses in all treatments. Additionally, all samples were neutralized at pH 6–8 prior to toxicity assessment.

Results and discussion

Optimization of photo-Fenton treatment

Preliminary experiments According to background chemistry, both Fe^{2+} and Fe^{3+} react with hydrogen peroxide through reactions involving radical intermediates (like $HO^{\bullet}$ and $HO_2^{\bullet}$) that can attack organic compounds (Eqs. (1)–(3)) (Evgenidou et al. 2007, Pignatello et al. 2006):

$$Fe^{2+} + H_2O_2 \rightarrow Fe^{3+} + OH^- + HO^{\bullet} \quad (1)$$

$$Fe^{3+} + H_2O_2 \rightarrow Fe\text{–}OOH^{2+} + H^+ \quad (2)$$

$$Fe\text{–}OOH^{2+} \rightarrow HO_2^{\bullet} + Fe^{2+} \quad (3)$$

In order to compare the effectiveness of the Fenton reaction with the photo-Fenton reaction, experiments were carried out under SSL by employing the Fe^{3+}/H_2O_2 system. It is well known that the irradiation of Fenton reaction systems with UV/visible light strongly accelerated the rate of degradation for a variety of pollutants due to the photochemical reduction of Fe(III) back to Fe(II) according to the following reaction:

$$Fe^{3+} + H_2O + h\nu \rightarrow Fe^{2+} + HO^{\bullet} + H^+ \quad (4)$$

As a result, irradiation of the Fenton reaction not only regenerates Fe(II), the catalytic species in the Fenton reaction (Eq. 4), but also produces additional hydroxyl radicals for the degradation of organic substrate. Thus, the photo-Fenton process is faster than the conventional thermal Fenton process.

Preliminary results for Fenton and photo-Fenton treatment of 5-FU using the solar simulator are summarized in Fig. 1. By Fenton treatment, only 15% elimination of the parent compound is achieved during the first 30 min, while at the same time the elimination caused by photo-Fenton treatment is

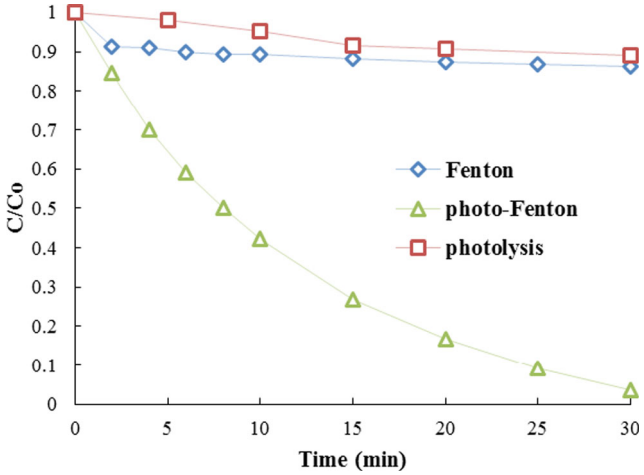

Fig. 1 Photo-Fenton treatment of 5-FU in comparison to Fenton treatment and direct photolysis; (C_o(5-FU) = 10 mg L^{-1}, C(Fe^{3+}) = 4.5 mg L^{-1}, C(H_2O_2) = 60 mg L^{-1})

approximately 96%; thus, further experiments have been focused on photo-Fenton processes. Direct photolysis (simulated solar radiation alone) was also studied, showing that only 2% of 5-FU was removed after 45 min of illumination (Fig. 1), indicating no significant contribution to the degradation of 5-FU.

Effect of 5-FU initial concentration

5-FU oxidation by photo-Fenton follows first-order kinetics according to the fitting high values of correlation coefficient, R^2 = 0.99. Photo-Fenton was applied, using various initial concentrations of 5-FU (1.5–10 mg L^{-1}), with a view to evaluate the effect of initial concentration of 5-FU to the photocatalytic rate (Fig. 2). The rest parameters were kept constant (Fe^{3+} concentration at 3 mg L^{-1} and H_2O_2 at 60 mg L^{-1}). Obviously, an increase in the concentration of 5-FU leads to a decrease in the photocatalytic rate constant that could be attributed to the lower ratio of active oxidative species to the substrate molecules. This behavior was similar to that reported for other studies (Lucas and Peres 2006, Modirshahla et al. 2007, Tamimi et al. 2008).

Effect of hydrogen peroxide concentration

The occurrence of adequate amounts of oxidant during the solar Fenton process is a crucial factor in regards to the continuation of the reactions and the mineralization of the drug (Velegraki & Mantzavinos 2015). The effect of the amount of hydrogen peroxide concentration to the degradation rate was examined by employing different initial concentrations of hydrogen peroxide ranged between 0 and 90 mg L^{-1}. 5-FU concentration and Fe^{3+} were kept constant at 10 and 3 mg L^{-1}. The results are presented in Fig. 2. It is obvious that the increase of the amount of hydrogen peroxide induces an increase of the reaction rate since more hydroxyl radicals are produced. This increase of the reaction rate continues up to a level which corresponds to an optimum concentration. However, at high dosages of the oxidant, a decrease of the degradation rate is observed, due to the hydroxyl radical scavenging effect of H_2O_2 (Eq. 5) and the recombination of hydroxyl radicals as well (Yamal-Turbay et al. 2013, Zazo et al. 2009).

$$H_2O_2 + HO^{\bullet} \rightarrow HO_2^{\bullet} + H_2O \quad (5)$$

Although other radicals (e.g., $HO_2^{\bullet}$) are produced, their oxidation potential is smaller than that of $HO^{\bullet}$ while the decomposition-deactivation of H_2O_2 to water and oxygen is also favored in the excess of H_2O_2.

Furthermore, even in the absence of the oxidant, degradation still occurs due to photolysis of $Fe_{(aq)}^{3+}$ according to Eq. 4. Indeed, at pH ≃ 3, the predominant Fe(III) species is the $[Fe^{III}OH(H_2O)_5]^{2+}$ complex which is able to undergo excitation throughout most of the ultraviolet spectral region. This excitation is followed by electron transfer producing Fe(II) aqua complex and $^{\bullet}OH$ radical (Poulain et al. 2003):

$$\left[Fe^{III}OH(H_2O)_5\right]^{2+} + H_2O + h\nu \rightarrow \left[Fe^{II}(H_2O)_6\right]^{2+} + HO^{\bullet} \quad (6)$$

Thus, based on the previous observations, the optimum concentration of H_2O_2 for photo-Fenton degradation of 5-FU corresponds to approximately 60 mg L^{-1}.

Effect of iron concentration

In order to examine the effect of iron on the degradation kinetics, experiments (5-FU concentration at 10 mg L^{-1} and H_2O_2 at 60 mg L^{-1}) were carried out at different initial concentrations of ferric ions (0–4.5 mg L^{-1}). The dependence of the constant rate on Fe^{3+} concentration is depicted in Fig. 2. In the absence of iron, a low reaction rate is observed (Fig. 2), due to the photolysis of peroxide (Irmak et al. 2004). By adding Fe^{3+} to the 5-FU solution, higher reaction rates are observed which can be attributed to enhanced H_2O_2 decomposition which in turn increases hydroxyl radical production (Velegraki & Mantzavinos 2015). A linear trend was observed up to ferric ion concentration of 4.5 mg L^{-1}. According to Eqs. (1–3), the amount of ferric ions added is proportional to the amount of ferrous ions which in turn is proportional to the amount of hydroxyl radicals produced and, consequently, to the degradation rate of 5-FU. At higher concentrations of ferric ions, the degradation rate increases only slightly due probably to restrictions posed by the available photons at the given irradiation intensity or by the excess of Fe(II) that could reduce the amount of $HO^{\bullet}$ radicals via the reaction:

$$Fe^{II} + HO^{\bullet} \rightarrow Fe^{III} + HO^{-} \quad (7)$$

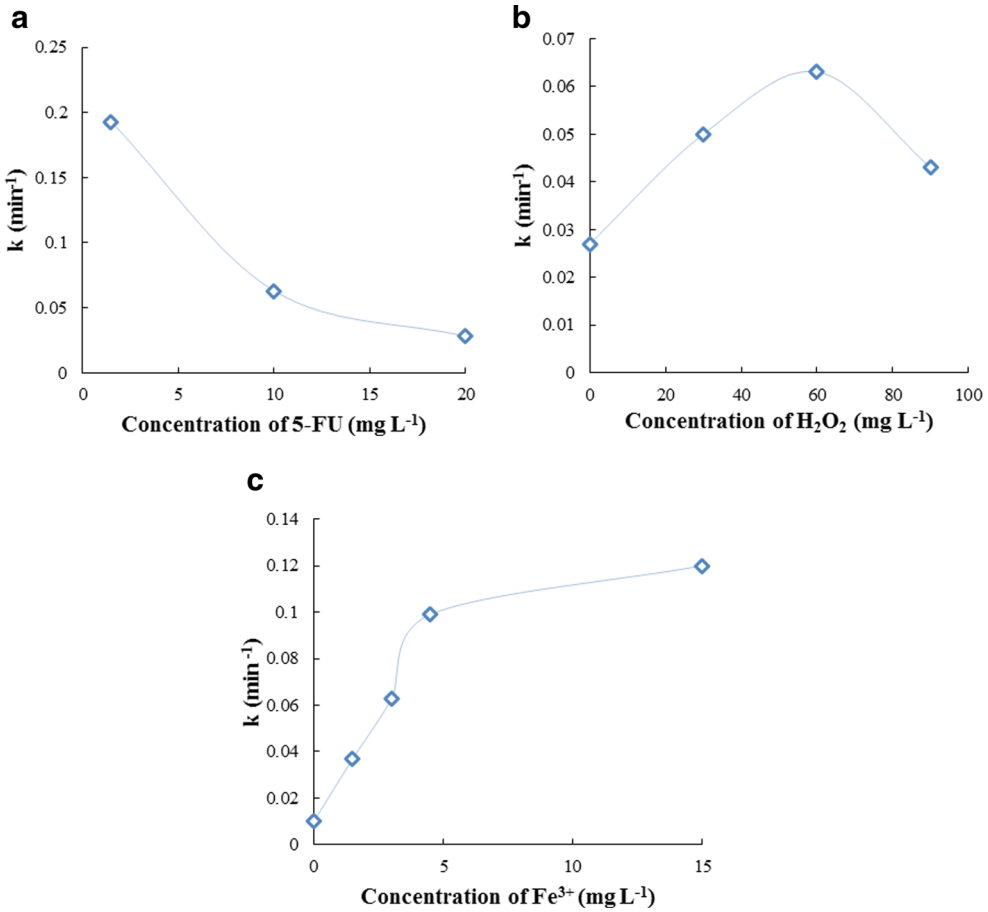

Fig. 2 The effect of operational parameters on 5-FU photo-Fenton degradation. **a** Effect of 5-FU loading ($C(Fe^{3+})$ = 3 mg L^{-1}, $C(H_2O_2)$ = 60 mg L^{-1}). **b** Effect of H_2O_2 loading (C_o(5-FU) = 10 mg L^{-1} ($C(Fe^{3+})$ = 3 mg L^{-1}). **c** Effect of Fe^{3+} loading (C_o(5-FU) = 10 mg L^{-1}, $C(H_2O_2)$ = 60 mg L^{-1}). *k* calculated for 10-min reaction

However, the residues of iron in treated effluent and settled sludge is harmful to the environment and needs further treatment to be separated (Gar Alalm et al. 2015). Consequently, lower concentrations that achieve a short reaction time without the requirement of further treatment for iron removal are preferable. For the reasons described above, the selected concentration of ferric ions for further experiments was 4.5 mg L^{-1}.

Comparison of Fenton and Fenton-like treatment of 5-FU

The efficiency of $Fe^{3+}/S_2O_8^{2-}$ system under solar irradiation for the degradation of 5-FU was studied and compared to the photo-Fenton (Fe^{3+}/H_2O_2) system. The ferrioxalate photo-Fenton reaction system was also investigated as it is known that the efficiency of the photo-Fenton process can be further enhanced by using organic carboxylic acids to complex Fe(III) (Pignatello et al. 2006). Oxalic to iron ratio is set to 1:3 to enable formation of the most stable complex ($[Fe(C_2O_4)_3^{3-}]$). A lower oxalate concentration would be inadequate, slowing down the ferrous iron regeneration rate, whereas an excess would act as hydroxyl radicals' scavenger (Doumic et al. 2015, Monteagudo et al. 2010). Thirty milligrams per liter of 5-FU was used in all cases, while concentration of ferric ions was 4.5 mg L^{-1}. In each case, the concentration of the oxidant was 100 mg L^{-1}.

Obviously, the addition of oxalic acid substantially improves the efficiency of photo-Fenton reaction, since the degradation of 5-FU is approximately 98% at the first 30 min of irradiation, while the rate constant is increased to 0.146 min^{-1} compared to 0.024 min^{-1} for the simple

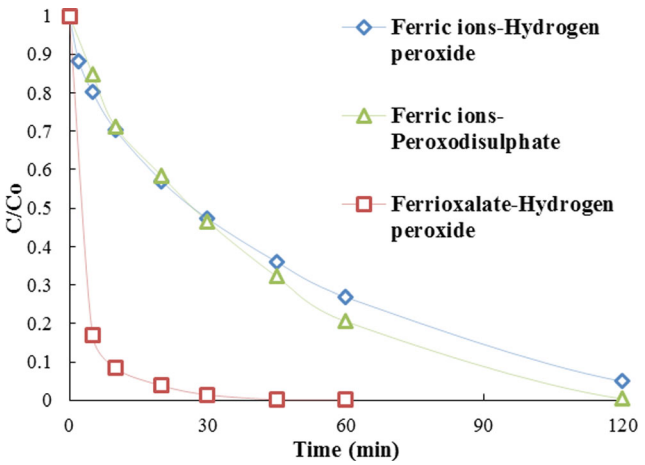

Fig. 3 Comparison of Fenton and Fenton-like treatment of 5-FU; (C_o(5-FU) = 30 mg L^{-1}, $C(Fe^{3+})$ = 4.5 mg L^{-1}, C(oxidant) = 100 mg L^{-1})

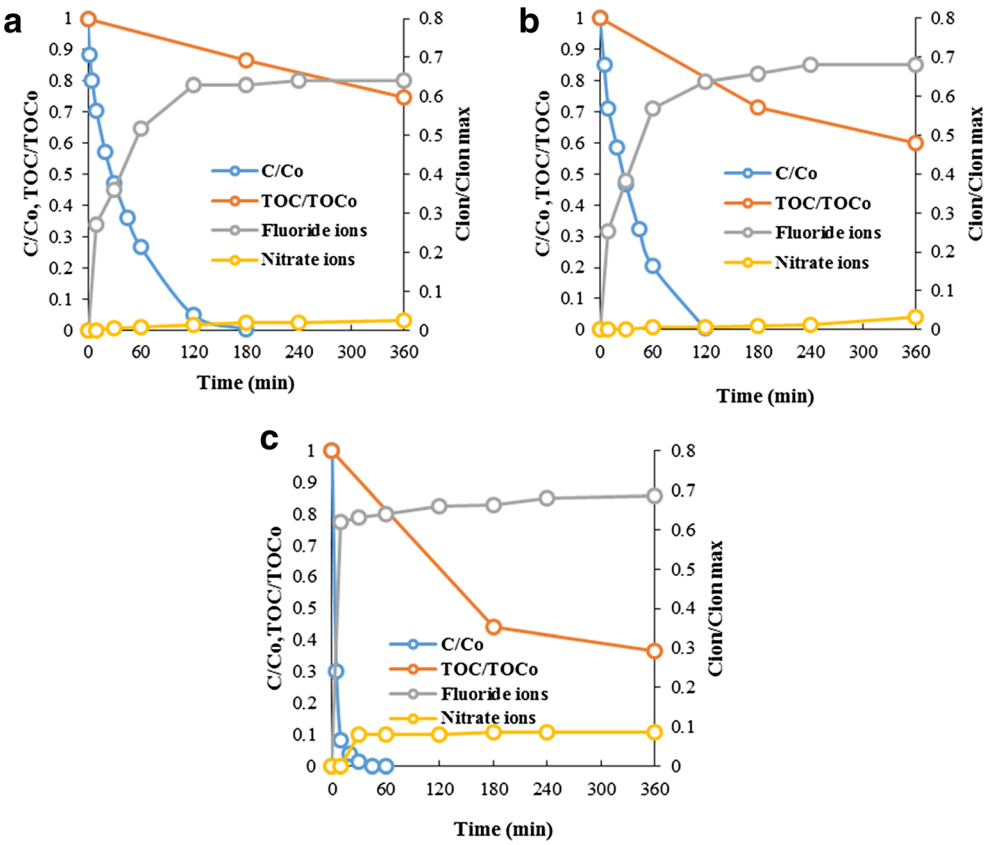

Fig. 4 Mineralization process of 5-FU. **a** SSL/Fe^{3+}/H_2O_2. **b** SSL/Fe^{3+}/$S_2O_8^{2-}$. **c** SSL/$[Fe(C_2O_4)_3]^{3-}$/H_2O_2; (C_o(5-FU) = 30 mg L^{-1}, C(Fe^{3+}) = 4.5 mg L^{-1}, C(oxidant) = 100 mg L^{-1})

photo-Fenton system (Fig. 3). DOC elimination is also substantially increased, from 25 to 64% (Fig. 4). This could be explained by the fact that H_2O_2 photolysis is not as efficient as ferrioxalate's complex ($[Fe(C_2O_4)_3]^{3-}$) photolysis. Ferrioxalate complexes can absorb light as far out as 570 nm, i.e., well expanded into the visible light region and they are decomposed efficiently (quantum yields of the order of unity) to Fe(II) and CO_2 (Chakma et al. 2015). On the contrary, H_2O_2 absorbs photons only below 350–400 nm (Monteagudo et al. 2008), which constitute only 3–5% of solar irradiation, because of its lower molar extinction.

As far as the comparison between Fe^{3+}/$S_2O_8^{2-}$ and Fe^{3+}/H_2O_2 systems is concerned, the kinetics for Fe^{3+}/$S_2O_8^{2-}$ reaction is clearly higher (0.04 min^{-1} for Fe^{3+}/$S_2O_8^{2-}$ and 0.024 min^{-1} for Fe^{3+}/H_2O_2). The data obtained from DOC measurements corroborate also the higher efficiency of Fe^{3+}/$S_2O_8^{2-}$ (Fig. 4). The DOC elimination of 5-FU after 6 h of irradiation is 25% for Fe^{3+}/H_2O_2 treatment and 40% for Fe^{3+}/$S_2O_8^{2-}$ treatment.

Table 1 High-resolution mass spectra data for 5-FU and identified TPs derived from LC-MS-TOF analysis

R_t (min)/code name	Pseudo-molecular ion formula	Theoretical m/z $[M-H]^-$	Experimental m/z $[M-H]^-$	Δ (ppm)	RDBE	Process
1.0/TP1	$C_4H_3N_2O_4$	143.0098	143.0103	−3.0	4.5	SSL/Fe^{3+}/$S_2O_8^{2-}$SSL/Fe^{3+}/H_2O_2 SSL/$[Fe(C_2O_4)_3]^{3-}$/H_2O_2
1.5/TP2*	$C_4H_3N_2O_3$	127.0149	127.0152	−2.3	4.5	SSL/Fe^{3+}/$S_2O_8^{2-}$
2.0/5-FU	$C_4H_2FN_2O_2$	129.0106	129.0105	0.3	4.5	
Rt (min)/code name	Pseudo-molecular ion formula	Theoretical m/z $[M+H]^+$	Experimental m/z $[M+H]^+$	Δ (ppm)	RDBE	Process
1.0/TP3	$C_4H_7N_2O_5$	163.0350	163.0352	−1.3	2.5	SSL/Fe^{3+}/H_2O_2
	$C_4H_5N_2O_4$	145.0244	145.0249	−3.8	3.5	SSL/Fe^{3+}/$S_2O_8^{2-}$
1.5/TP2*	$C_4H_5N_2O_3$	129.0295	129.0296	−0.9	3.5	SSL/Fe^{3+}/$S_2O_8^{2-}$
2.0/5-FU*	$C_4H_4FN_2O_2$	131.0251	131.0254	−1.8	3.5	

Asterisks indicate compounds detected in both positive and negative ionization modes

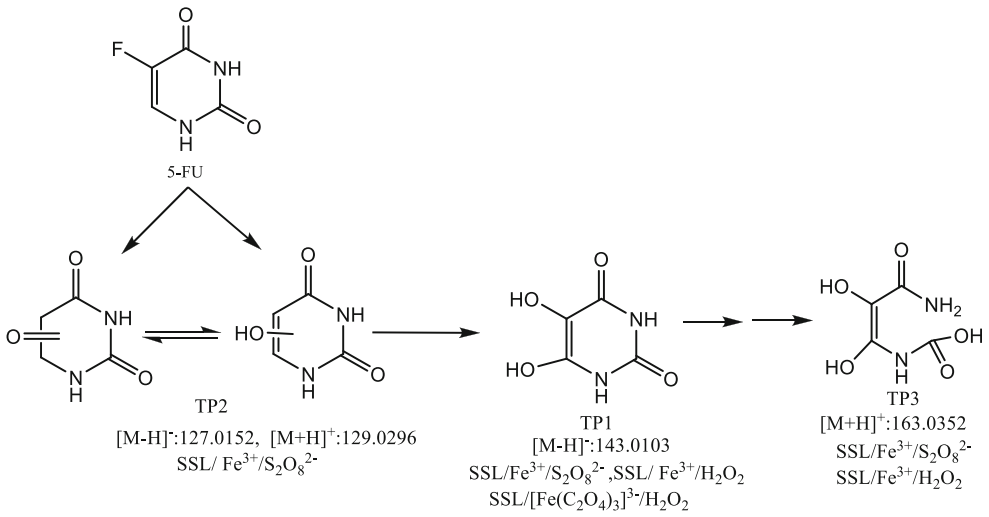

Fig. 5 Transformation pathways of 5-FU under SSL/Fe^{3+}/H_2O_2, SSL/Fe^{3+}/$S_2O_8^{2-}$, and SSL/$[Fe(C_2O_4)_3]^{3-}$/H_2O_2 processes ($[M-H]^-$/$[M+H]^+$: experimental m/z mass)

Identification of transformation products and toxicity evolution

Accurate mass measurements, derived by LC-TOF-MS analysis in both positive and negative ionization mode, provided the identification and structural elucidation of the TPs, generated during the applied AOPs. All the high resolution accurate LC-MS data of the parent compound and the identified TPs are summarized in Table 1. Based on the accurate mass measurements, the proposed transformation mechanism of 5-FU was depicted in Fig. 5. The effective transformation of 5-FU was initiated by $HO^{\bullet}$ radical attack on the C-F bond of the parent molecule and followed by subsequent substitution of fluorine atom

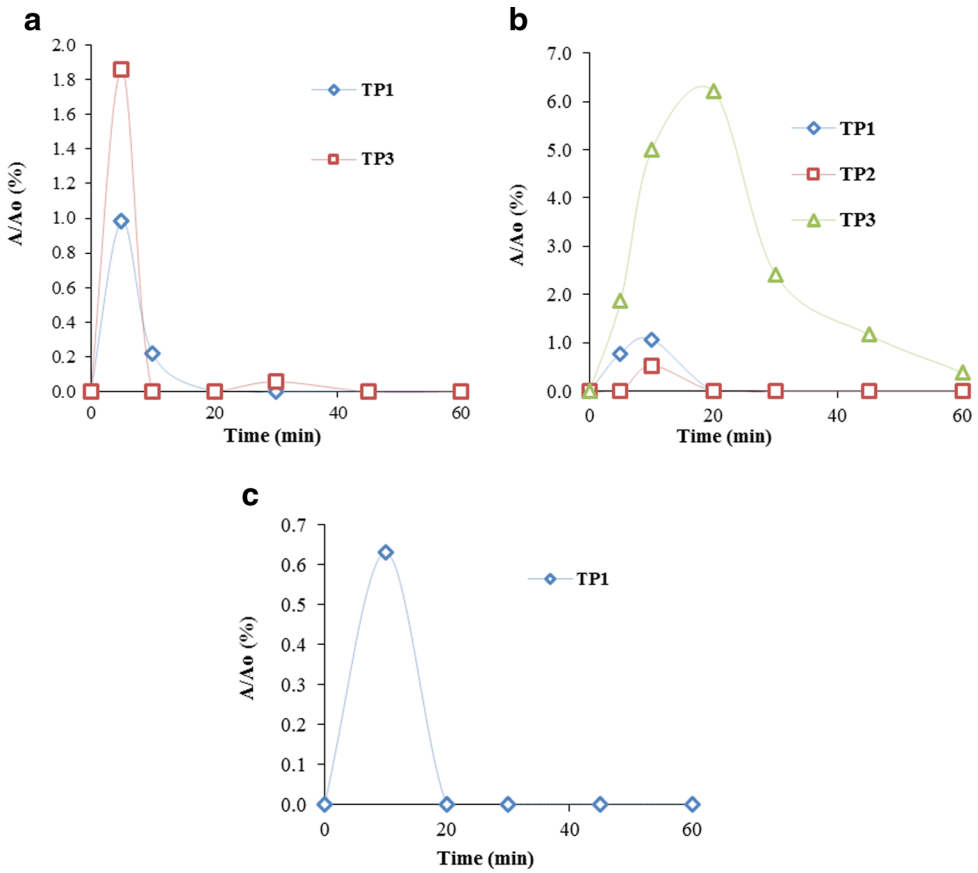

Fig. 6 Kinetics of 5-FU transformation products. **a** SSL/Fe^{3+}/H_2O_2. **b** SSL/Fe^{3+}/$S_2O_8^{2-}$. **c** SSL/$[Fe(C_2O_4)_3]^{3-}$/H_2O_2; (C_o(5-FU) = 30 mg L^{-1}, C(Fe^{3+}) = 4.5 mg L^{-1}, C(oxidant) = 100 mg L^{-1}, A_o = initial 5-FU peak area)

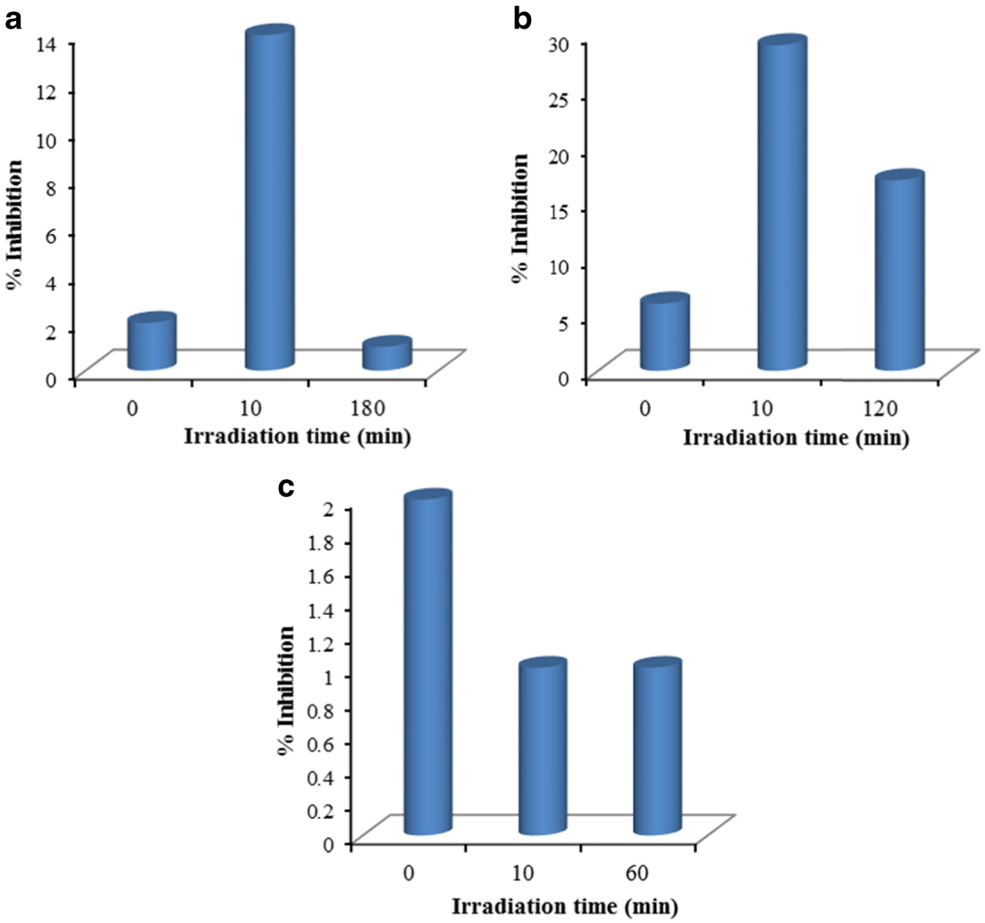

Fig. 7 Toxicity evolution as a function of photocatalytic treatment. **a** SSL/Fe^{3+}/H_2O_2. **b** SSL/Fe^{3+}/$S_2O_8^{2-}$. **c** SSL/$[Fe(C_2O_4)_3]^{3-}$/H_2O_2; (Co(5-FU) = 30 mg L^{-1}, C(Fe^{3+}) = 4.5 mg L^{-1}, C(oxidant) = 100 mg L^{-1})

by OH group, leading to the formation of TP2. As previously reported, TP2 has also been detected during the hydrolysis of 5-FU in aqueous solutions under alkaline conditions (Legay et al. 2014). In accordance with our results, defluorination followed by hydroxylation has been characterized as a common transformation pathway of fluorinated organic compounds during their treatment by different AOPs (An et al. 2010, Minero et al. 1991, Sturini et al. 2012). Subsequent oxidant attack of $HO^{\bullet}$ radicals to the aromatic ring leads to TP1, a polyhydroxylated derivative of defluorinated 5-FU, which was identified in all the studied processes and proved the significant role of $HO^{\bullet}$ radicals. Successive polyhydroxylation is followed by the cleavage of the aromatic heterocyclic ring and the formation of the TP3 with a probable structure of carboxylic acid derivative.

The proposed transformation pathways are similar but not identical to those reported during the degradation of 5-FU by photolysis and different AOPs (Elsellami et al. 2014, Lutterbeck et al. 2015b, 2016). The identified TPs proved that oxidant attack of the $HO^{\bullet}$ radical on the C-F bond and subsequently substitution of fluorine by OH group is the major pathway. For further elucidation of the possible transformation pathway, the kinetic profiles of the identified TPs were followed. The evolution profiles of TPs, i.e., % peak area ratio (A/A_0, where A is the TP peak area and A_0 is the peak area of 5-FU at 0 min) vs time, are presented in Fig. 6. All identified TPs were rapidly degraded while maximum concentrations of TP1 and TP2 were recorded within the first 10 min, pointing out the parallel formation of defluorinated and monohydroxylated as well as di-hydroxylated derivatives. The generation of the ring-opened TP3 maximized at 20 min showing the successive steps after defluorination and polyhydroxylation of 5-FU molecule. Despite the rapid degradation of 5-FU and the generated TPs, the DOC removal was rather slow for all oxidation techniques (30–50% decrease after 360 min), except from ferrioxalate's complex process, which reaches almost 65% decrease after 360 min.

The slow rate of mineralization implies the formation of deep oxidation TPs as a consequence of successive ring opening and further oxidation-dealkylation of the identified TPs. Based on the structure of 5-FU, aliphatic organic acids such as oxalic acid, tartronic acid, and mesoxalic acid can be considered as final products, before complete mineralization (Elsellami et al. 2014).

V. fischeri toxicity bioassay was also conducted, in order to evaluate the potent toxicity of the TPs formed during the applied AOPs. As presented in Fig. 7, the original solution at

30 mg L^{-1} in ultrapure water without irradiation exhibited low toxicity to *V. fischeri* (2–6% inhibition). In contrast, the toxicity increased during the first stages of the photocatalytic reaction, reaching the inhibition value of about 15 and 30% for SSL/Fe^{3+}/H_2O_2 and SSL/Fe^{3+}/$S_2O_8^{2-}$ treatments. At this time, the TPs formed are still present in the solution. Consequently, the toxicity profile indicates that the TPs' content during the photocatalytic procedure exhibits more toxic effects than the parent compound for those two treatments. However, the toxicity levels at the end of its treatment are lower than the toxicity levels at the first stages of the photocatalytic reaction. On the other hand, SSL/$[Fe(C_2O_4)_3]^{3-}$/H_2O_2 treatment presented almost zero toxicity at all stages of the photocatalytic reaction. This is probably because the degradation procedure is quite faster and the TPs responsible for the toxicity in the other two treatments have been eliminated in short times. Generally, the toxicity of 5-FU and its TPs was very low at these concentration levels which are in agreement with previous studies on 5-FU and its TPs' acute toxicity (Lutterbeck et al. 2015b, 2016).

Conclusions

In this study, new data are presented about the degradation and total mineralization of 5-FU using photo-Fenton and Fenton-like processes. The degradation efficiency was found to be enhanced by the addition of oxidants and the decrease of the initial concentration of 5-FU. A comparison between the applied processes showed that the ferrioxalate system was more efficient for the degradation and mineralization of 5-FU. Under the studied processes, the transformation of 5-FU proceeded through deflurination, hydroxylation, and ring-opening pathways, involving hydroxyl radical attack on C-F bond and aromatic ring. All the identified intermediates were easily degraded within 20–60 min of treatment. Toxicity assessment revealed that both 5-FU and the treated samples exhibited relatively low toxicity to *V. fischeri*. According to the obtained results, the efficiency of photo-Fenton and Fenton-like processes to remove 5-FU from aqueous phase, avoiding the formation of highly toxic TPs, was demonstrated.

Acknowledgments The analytical part of this work has been co-financed by the European Union (European Social Fund—ESF) and Greek national funds through the Operational Program "Education and Lifelong Learning" of the National Strategic Reference Framework (NSRF)—Research Funding Program "Excellence II (Aristeia II)," Research Grant No. 4199, which is gratefully acknowledged.

References

An T, Yang H, Song W, Li G, Luo H, Cooper WJ (2010) Mechanistic considerations for the advanced oxidation treatment of fluoroquinolone pharmaceutical compounds using TiO2 heterogeneous catalysis. J Phys Chem A 114:2569–2575

Antonopoulou M, Konstantinou I (2014) Photocatalytic treatment of metribuzin herbicide over TiO2 aqueous suspensions: removal efficiency, identification of transformation products, reaction pathways and ecotoxicity evaluation. J Photochem Photobiol A Chem 294:110–120

Antonopoulou M, Karagianni P, Konstantinou IK (2016) Kinetic and mechanistic study of photocatalytic degradation of flame retardant Tris (1-chloro-2-propyl) phosphate (TCPP). Appl Catal B Environ 192:152–160

Besse J-P, Latour J-F, Garric J (2012) Anticancer drugs in surface waters: what can we say about the occurrence and environmental significance of cytotoxic, cytostatic and endocrine therapy drugs? Environ Int 39:73–86

Brezovšek P, Eleršek T, Filipič M (2013) The effects of selected cytostatics and their mixtures on aquatic primary producers. Toxicology letters 221, Supplement, S96

Brezovšek P, Eleršek T, Filipič M (2014) Toxicities of four anti-neoplastic drugs and their binary mixtures tested on the green alga Pseudokirchneriella subcapitata and the cyanobacterium *Synechococcus leopoliensis*. Water Res 52:168–177

Catastini C, Mullot JU, Boukari S, Mazellier P, Levi Y, Cervantes P, Ormsby JN (2008) Assessment of antineoplastic drugs in effluents of two hospitals. Journal Europeen d'Hydrologie 39:171–180

Chakma S, Das L, Moholkar VS (2015) Dye decolorization with hybrid advanced oxidation processes comprising sonolysis/Fenton-like/photo-ferrioxalate systems: a mechanistic investigation. Separation and Purification Technology 156, Part 2:596–607

De la Cruz N, Giménez J, Esplugas S, Grandjean D, De Alencastro LF, Pulgarín C (2012) Degradation of 32 emergent contaminants by UV and neutral photo-Fenton in domestic wastewater effluent previously treated by activated sludge. Water Res 46:1947–1957

Doumic LI, Soares PA, Ayude MA, Cassanello M, Boaventura RAR, Vilar VJP (2015) Enhancement of a solar photo-Fenton reaction by using ferrioxalate complexes for the treatment of a synthetic cotton-textile dyeing wastewater. Chem Eng J 277:86–96

Elsellami L, Sahel K, Dappozze F, Horikoshi S, Houas A, Guillard C (2014) Titania-based photocatalytic degradation of two nucleotide bases, cytosine and uracil. Appl Catal A Gen 485:207–213

Evgenidou E, Konstantinou I, Fytianos K, Poulios I (2007) Oxidation of two organophosphorous insecticides by the photo-assisted Fenton reaction. Water Res 41:2015–2027

Ferrando-Climent L, Rodriguez-Mozaz S, Barceló D (2014) Incidence of anticancer drugs in an aquatic urban system: from hospital effluents through urban wastewater to natural environment. Environ Pollut 193:216–223

Ferrando-Climent L, Cruz-Morató C, Marco-Urrea E, Vicent T, Sarrà M, Rodriguez-Mozaz S, Barceló D (2015) Non conventional biological treatment based on Trametes versicolor for the elimination of recalcitrant anticancer drugs in hospital wastewater. Chemosphere 136:9–19

Gar Alalm M, Tawfik A, Ookawara S (2015) Comparison of solar TiO2 photocatalysis and solar photo-Fenton for treatment of pesticides industry wastewater: operational conditions, kinetics, and costs. Journal of Water Process Engineering 8:55–63

Giannakis S, Gamarra Vives FA, Grandjean D, Magnet A, De Alencastro LF, Pulgarin C (2015) Effect of advanced oxidation processes on the micropollutants and the effluent organic matter contained in municipal wastewater previously treated by three different secondary methods. Water Res 84:295–306

Ikehata K, Jodeiri Naghashkar N, Gamal El-Din M (2006) Degradation of aqueous pharmaceuticals by ozonation and advanced oxidation processes: a review. Ozone Sci Eng 28:353–414

Irmak S, Kusvuran E, Erbatur O (2004) Degradation of 4-chloro-2-methylphenol in aqueous solution by UV irradiation in the presence of titanium dioxide. Appl Catal B Environ 54:85–91

Kosjek T, Perko S, Žigon D, Heath E (2013) Fluorouracil in the environment: analysis, occurrence, degradation and transformation. J Chromatogr A 1290:62–72

Kovács R et al (2015) Assessment of toxicity and genotoxicity of low doses of 5-fluorouracil in zebrafish (*Danio rerio*) two-generation study. Water Res 77:201–212

Legay R, Massou S, Azéma J, Martino R, Malet-Martino M (2014) Hydrolytic pathway of 5-fluorouracil in aqueous solutions for clinical use. J Pharm Biomed Anal 98:446–462

Lin HH-H, Lin AY-C (2014) Photocatalytic oxidation of 5-fluorouracil and cyclophosphamide via UV/TiO2 in an aqueous environment. Water Res 48:559–568

Lin AY, Wang XH, Lee WN (2013) Phototransformation determines the fate of 5-fluorouracil and cyclophosphamide in natural surface waters. Environ Sci Technol 47:4104–4112

Lucas MS, Peres JA (2006) Decolorization of the azo dye Reactive Black 5 by Fenton and photo-Fenton oxidation. Dyes Pigments 71:236–244

Lutterbeck CA, Kern DI, Machado ÊL, Kümmerer K (2015a) Evaluation of the toxic effects of four anti-cancer drugs in plant bioassays and its potency for screening in the context of waste water reuse for irrigation. Chemosphere 135:403–410

Lutterbeck CA, Wilde ML, Baginska E, Leder C, Machado ÊL, Kümmerer K (2015b) Degradation of 5-FU by means of advanced (photo)oxidation processes: UV/H2O2, UV/Fe2 +/H2O2 and UV/TiO2—comparison of transformation products, ready biodegradability and toxicity. Sci Total Environ 527–528:232–245

Lutterbeck CA, Wilde ML, Baginska E, Leder C, Machado ÊL, Kümmerer K (2016) Degradation of cyclophosphamide and 5-fluorouracil by UV and simulated sunlight treatments: assessment of the enhancement of the biodegradability and toxicity. Environmental pollution 208, Part B, 467–476

Mahnik SN, Lenz K, Weissenbacher N, Mader RM, Fuerhacker M (2007) Fate of 5-fluorouracil, doxorubicin, epirubicin, and daunorubicin in hospital wastewater and their elimination by activated sludge and treatment in a membrane-bio-reactor system. Chemosphere 66:30–37

Minero C, Aliberti C, Pelizzetti E, Terzian R, Serpone N (1991) Kinetic studies in heterogeneous photocatalysis. 6. AM1 simulated sunlight photodegradation over titania in aqueous media: a first case of fluorinated aromatics and identification of intermediates. Langmuir : the ACS journal of surfaces and colloids 7:928–936

Miolo G, Marzano C, Gandin V, Palozzo AC, Dalzoppo D, Salvador A, Caffieri S (2011) Photoreactivity of 5-fluorouracil under UVB light: photolysis and cytotoxicity studies. Chem Res Toxicol 24:1319–1326

Modirshahla N, Behnajady MA, Ghanbary F (2007) Decolorization and mineralization of C.I. Acid Yellow 23 by Fenton and photo-Fenton processes. Dyes Pigments 73:305–310

Monteagudo JM, Durán A, López-Almodóvar C (2008) Homogeneus ferrioxalate-assisted solar photo-Fenton degradation of Orange II aqueous solutions. Appl Catal B Environ 83:46–55

Monteagudo JM, Durán A, Aguirre M, Martín IS (2010) Photodegradation of Reactive Blue 4 solutions under ferrioxalate-assisted UV/solar photo-Fenton system with continuous addition of H2O2 and air injection. Chem Eng J 162:702–709

Papoutsakis S, Afshari Z, Malato S, Pulgarin C (2015) Elimination of the iodinated contrast agent iohexol in water, wastewater and urine matrices by application of photo-Fenton and ultrasound advanced oxidation processes. J Environ Chem Eng 3:2002–2009

Parrella A, Lavorgna M, Criscuolo E, Russo C, Fiumano V, Isidori M (2014a) Acute and chronic toxicity of six anticancer drugs on rotifers and crustaceans. Chemosphere 115:59–66

Parrella A, Lavorgna M, Criscuolo E, Russo C, Isidori M (2014b) Estrogenic activity and cytotoxicity of six anticancer drugs detected in water systems. Sci Total Environ 485–486:216–222

Parrella A, Lavorgna M, Criscuolo E, Russo C, Isidori M (2015) Ecogenotoxicity of six anticancer drugs using comet assay in daphnids. J Hazard Mater 286:573–580

Pignatello JJ, Oliveros E, MacKay A (2006) Advanced oxidation processes for organic contaminant destruction based on the Fenton reaction and related chemistry. Crit Rev Environ Sci Technol 36:1–84

Poulain L, Mailhot G, Wong-Wah-Chung P, Bolte M (2003) Photodegradation of chlortoluron sensitised by iron(III) aquacomplexes. J Photochem Photobiol A Chem 159:81–88

Straub JO (2010) Combined environmental risk assessment for 5-fluorouracil and capecitabine in Europe. Integr Environ Assess Manag 6:540–566

Sturini M, Speltini A, Maraschi F, Profumo A, Pretali L, Irastorza EA, Fasani E, Albini A (2012) Photolytic and photocatalytic degradation of fluoroquinolones in untreated river water under natural sunlight. Appl Catal B Environ 119–120:32–39

Tamimi M, Qourzal S, Barka N, Assabbane A, Ait-Ichou Y (2008) Methomyl degradation in aqueous solutions by Fenton's reagent and the photo-Fenton system. Sep Purif Technol 61:103–108

Toolaram AP, Kümmerer K, Schneider M (2014) Environmental risk assessment of anti-cancer drugs and their transformation products: a focus on their genotoxicity characterization-state of knowledge and short comings. Mutat Res Rev Mutat Res 760:18–35

Velegraki T, Mantzavinos D (2015) Solar photo-Fenton treatment of winery effluents in a pilot photocatalytic reactor. Catalysis Today 240, Part A, 153–159

Weber J, Halsall CJ, Wargent JJ, Paul ND (2009) A comparative study on the aqueous photodegradation of two organophosphorus pesticides under simulated and natural sunlight. J Environ Monit 11(3):654–659

Weissbrodt D, Kovalova L, Ort C, Pazhepurackel V, Moser R, Hollender J, Siegrist H, McArdell CS (2009) Mass flows of x-ray contrast media and cytostatics in hospital wastewater. Environ Sci Technol 43:4810–4817

Yamal-Turbay E, Jaén E, Graells M, Pérez-Moya M (2013) Enhanced photo-Fenton process for tetracycline degradation using efficient hydrogen peroxide dosage. J Photochem Photobiol A Chem 267:11–16

Zazo JA, Casas JA, Mohedano AF, Rodriguez JJ (2009) Semicontinuous Fenton oxidation of phenol in aqueous solution. A kinetic study Water research 43:4063–4069